

Impact of gravity waves on the middle atmosphere of Mars studied combining Global Climate modelling and Mars Climate Sounder observations

G. Gilli (1,2), F. Forget (2), A. Spiga (2), T. Navarro (3), L. Montabone (3,2)

(1) Instituto de Astrofísica e Ciências do Espaço (IA), Lisbon, Portugal, (2) Laboratoire de Météorologie Dynamique (LMD), Paris, France, (3) Department of Earth, Planetary, and Space Sciences, University of California, Los Angeles, USA (3) Space Science Institute (SSI), Boulder, CO, USA. (ggilli@oal.ul.pt)

Abstract

We implemented a stochastic parameterization of non-orographic gravity waves (GW) into the Laboratoire de Météorologie Dynamique (LMD) Mars General Circulation Model (LMD-MGCM), following an innovative approach as described in [1]. The source is assumed to be located above typical convective cells (≈ 250 Pa) and the impact of GW on the circulation and the predicted thermal structure above 50 km is analyzed. We focus on the comparison between model simulations and observations by the Mars Climate Sounder (MCS) on board Mars Reconnaissance Orbiter [2] during Martian Year (MY) 29. The inclusion of the parametrized gravity waves significantly improve the accuracy of the LMD-MGCM in comparison with the observations, thus providing a plausible explanation to the systematic biases previously identified between 1 and 0.01 Pa (around 50-80 km), locally reaching 10 to 20 K. The corresponding changes in mean zonal wind velocity reach 100 m/s in proximity of the equatorial easterly jet.

1. Introduction

Gravity waves (GWs) are frequently detected in terrestrial planet atmospheres and they are supposed to play a dominant role in their large-scale circulation and variability. Small scale variability, in the form of perturbations of density and temperature have systematically been observed in the upper atmosphere of Mars whenever in situ data have been obtained [3, 5, 4] and attributed to GWs. In particular, non-orographic (i.e non-zero phase velocity) GW are supposed to be emitted above the convective layer and propagate upwards, providing a significant source of momentum and energy, thus affecting the transport of heat and constituents. The role of mesoscale GW is also supposed

to be crucial for local CO₂ condensation, responsible of the formation of mesospheric CO₂ clouds observed by Mars Express between 60 and 80 km altitude [6]. Thermal effects of gravity waves has been proposed to explain some of the puzzling model-observation discrepancy identified in the Martian atmosphere temperatures between 100 and 140 km [7]

c [m/s]	k_h [km]	F^0 kg m ⁻¹ s ⁻²	S_c
[1 - 30]	[10 - 300]	[0 - 10 ⁻⁴]	1

Table 1: Baseline wave characteristics in the GW scheme implemented in this work: c the absolute phase speed, k_h the horizontal wavelength amplitude, F^0 the vertical momentum (EP-flux) at the source (≈ 8 km), S_c the saturation parameter. Values in the bracket indicate the extremes of the probability distribution used in the "best-case" simulations.

2. This work

One of the main goals of this study is to understand the role of non-orographic GW on the global circulation and the thermal structure of the Martian middle atmosphere (50-100 km altitude). What is the magnitude of GW-induced drag on the winds? Can GW explain the remaining discrepancy between the MCS observations and the GCM simulations? If so, what is their impact on the predicted winds? With these purposes in mind we use the LMD-MGCM, a finite-difference model based on the discretization of the horizontal domain fields on a latitude-longitude grid [8], being 64 longitude x 48 latitudes (3.75° x 5.62°) the horizontal resolution used in this work. We have employed the latest version of the model which includes several recent improvements [9] in addition to the implementation of a non-orographic GW parameterization follow-

ing the formalism developed for the Earth GCM fully described in [1]. We focus here on the comparison between model simulations and observations by the Mars Climate Sounder (MCS) on board MRO [2] during the MY29. MCS represents the best existing systematic measurements of the Martian mesosphere up to 80 km. Discrepancies between data and model, notably the incorrect representation of thermal tide wave in the vertical, such as those found with the MCS observations [9, 10], indicated that some key process(es) are missing in our model.

2.1 Non-orographic GW parameterization

The GW scheme is based on a stochastic approach, in which a finite number M of waves with characteristics chosen randomly, but within a fixed probability distribution, are launched upwards at each time-step from a few random location to simulate they global effect. We assumed that the GW source is placed above typical convective cells (i.e around 8 km, depending on the topography). This allows to treat a large number of waves at a given time t by adding the effect of those M waves to that of the waves launched at previous steps, to compute the tendencies. A range of plausible values, and for different representations of the mean flow thermal forcing, have been considered (Gilli et al. 2018, in preparation).

3. Impact of GW mean flow forcing parameters

The main tunable GW parameters used in our scheme are listed in Table 1. The GW induced drag drives changes of the wind (e.g. deceleration/acceleration of jet streams) and consequently produces thermal structure variations via adiabatic heating/cooling rates associated with the altered circulation. An example of sensitivity tests, performed to evaluate the impact of GW mean flow forcing to thermal tides is shown in Figure 1. Those tests also help to select the baseline parameters by MCS-MGCM comparison. As shown in the Figure: 1) the maximum day-night difference value in Panel C ("best-case") is around 20 K, comparable with observed values, and more interestingly 2) the peak altitude of the tides is shifted down, and 3) its amplitude is also more realistic (between 22°S and 22°N latitudes, as observed) The impact of induced GW drag on the jet streams for all martian seasons will be also shown and discussed.

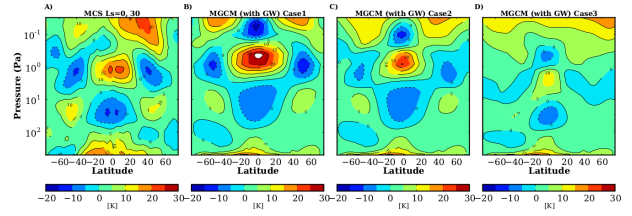


Figure 1: Example of observed and simulated day-night temperature differences (in K), between dayside (15 LT) and nightside (3 LT), during $L_s = 0^\circ\text{--}30^\circ\text{N}$. Panel A: MCS measurements. Panels B, C and D: selection of model simulations. Panel C represents the "best-case" run (Table 1). Panels B and D show two tests, where the upper value of the probability distribution for the EP-flux at the source is reduced and increased by one order of magnitude, respectively.

Acknowledgements

GG was supported by FCT (Portugal) through national funds and from FEDER through COMPETE2020 by grants UID/FIS/04434/2013, POCI-01-0145-FEDER-007672, PTDC/FIS-AST/1526/2014 and POCI-01-0145-FEDER-016886

References

- [1] Lott, F., and L. Guez (2013), J. Geophys. Res. (Atmospheres), *118*, 8897–8909.
- [2] McCleese et al. 2010, J. Geophys. Res. (Planets), *115*(E14), E12016
- [3] Fritts et al. 2006, J. of Geophys. Res. (Space Physics), *111*, A12304,
- [4] Terada et al. 2017, J. of Geophys. Res. (Space Physics), *122*, 2374–2397
- [5] Yiğit et al. 2015, Geophys. Res. Letter, *42*, 8993–9000
- [6] Spiga et al. 2012, Geophys. Res. Letters, *39*, L02201
- [7] Medvedev et al. 2015, J. Geophys. Res. (Planets), *120*, 913–927,
- [8] Forget et al. 1999, J. Geophys. Res., *104*, 24,155–24,176.
- [9] Forget et al. 2017, in *The Mars Atmosphere: Modelling and observation*, edited by F. Forget and M. Millour, p. 1113.
- [10] Navarro et al. 2017, *Earth and Space Science*, *4*(12), 690–722,